

# Deuterium and oxygen isotopes, paleoelevations of the Sierra Nevada, and Cenozoic climate

Peter Molnar<sup>†</sup>

Department of Geological Sciences, Cooperative Institute for Research in Environmental Sciences (CIRES), University of Colorado, Boulder, Colorado 80309-0399, USA

## ABSTRACT

Although geomorphic observations suggest that the Sierra Nevada has tilted so that the crest has risen 1–2 km since late Miocene time, deuterium and oxygen-18 isotope concentrations in Cenozoic geologic materials decrease eastward across California and Nevada similarly to those in modern, orographically induced precipitation, as if little change in Sierra Nevada elevations has occurred since Eocene time. Orographic precipitation, however, depends on the amount of moisture in the atmosphere, which in turn can be much larger in warm air, as in Eocene or Oligocene time and in summer, than in the cooler air characteristic of present-day, dominantly winter, precipitation. Moreover, the integrated rainout of vapor, and hence presumably in stable isotope concentrations in the remaining vapor, depends largely on the difference in heights traversed by air masses, not slopes of mountain ranges. Thus, if due simply to orographically induced rainout, both Eocene and Oligocene variations in deuterium isotopes across the Sierra Nevada and Miocene–Quaternary differences in deuterium and oxygen isotopes between the Great Valley of California and the Basin and Range place only weak constraints on the slope or past elevations of the Sierra Nevada. They do not necessarily contradict the inference that the crest of the Sierra Nevada has risen 1000 m or more since late Miocene time.

## INTRODUCTION

East-west topographic profiles across the Sierra Nevada of California show a gentle slope to the west as if a block of crust has rotated about a horizontal axis parallel to the range, with the crest of the range having risen relative to the floor of the Great Valley of California. In the northern Sierra, Eocene

gravel deposits define ancient valleys that can be traced westward from elevations >2000 m to the Great Valley and that seem to have been characterized by gentle longitudinal profiles (Fig. 1). The difference between the characteristic regional slope and the gentler profile of the ancient Yuba River led Lindgren (1911) to infer that the high peaks of the Sierra owe their current elevations to such tilting. Although some have questioned the magnitude of tilting (e.g., Hudson, 1955), most subsequent studies have refined and corroborated Lindgren's inference (e.g., Christensen, 1966; Huber, 1981, 1990; Jones et al., 2004; Small and Anderson, 1995; Unruh, 1991; Wakabayashi and Sawyer, 2001). Jones et al. (2004), in particular, showed that when slopes of the ancient valleys are plotted against the orientation of the valleys, segments that flowed westward are now steeper than those that flowed northward or southward. This pattern is easily explained by a tilting of the ancient channels about an axis trending roughly north-south, parallel to the present-day Sierra Nevada.

Efforts to date when such tilting occurred have repeatedly produced evidence suggesting that late Miocene to Pliocene tilting accounts for at least part (1–2 km) of the present-day height of the Sierran crest (e.g., Christensen, 1966; Dalrymple, 1963; Huber, 1981, 1990; Hudson, 1960; Unruh, 1991; Wakabayashi and Sawyer, 2001). Moreover, rapid incision into parts of the Sierra Nevada seems to have begun near 3 Ma, and Stock et al. (2004, 2005) argued that these increased incision rates reflect tilting of the Sierra, not climate change. Recently, however, others have exploited stable isotopes derived from precipitation in the atmosphere to challenge this timing.

When water vapor condenses, heavy isotopes, such as deuterium or <sup>18</sup>O, enter the liquid phase more readily than the lighter isotopes, so that when the condensate precipitates, the atmosphere becomes depleted in the heavy isotopes (e.g., Dansgaard, 1964; Gat, 1996; Rowley et al., 2001; Rozanski et al., 1992). As an air mass moves from over an ocean with an abundant

supply of moisture, onto a continent, and then over a mountain range, condensation and precipitation will deplete the vapor of heavy isotopes (e.g., Friedman and Smith, 1970; Scholl et al., 2007). In the absence of resupply of moisture, eventually the precipitation will contain only a small concentration of heavy isotopes (e.g., Chamberlain and Poage, 2000; Poage and Chamberlain, 2001). Orography concentrates precipitation on the windward side of rising terrain; as moist air is forced upward, it cools adiabatically, and when the temperature drops sufficiently, the air becomes saturated, vapor condenses, clouds form, and precipitation occurs. As Friedman and Smith (1970), Mulch et al. (2008), and others have shown, for modern precipitation, and Kendall and Coplen (2001) for stream water, eastward decreases in both deuterium and <sup>18</sup>O content occur largely over the Sierra Nevada where precipitation is highest.

Several authors have exploited this logic and measurements of deuterium or oxygen isotopes,  $\delta D$  or  $\delta^{18}O$ , to place constraints on past elevations, not just of the Sierra Nevada. I review relevant studies and relevant simple theories of orographic precipitation, and I then offer another interpretation in which the similarity of present-day and past spatial variations in stable isotopes could result from a combination of different elevation profiles and different climatic conditions.

## INFERENCES OF PALEOELEVATIONS OF THE SIERRA NEVADA FROM STABLE ISOTOPES

Poage and Chamberlain (2002) measured values of oxygen isotopes,  $\delta^{18}O$ , from authigenic calcite and smectite samples and other minerals that had weathered from middle Miocene to late Pliocene volcanic ash in the western Basin and Range Province (Fig. 1). They showed that the measured values would be in equilibrium with present-day precipitation. They concluded that the Sierra Nevada must have provided a rain shadow in Miocene time comparable to that

<sup>†</sup>E-mail: peter.molnar@colorado.edu

today, and that the crest of the range may have decreased, not increased, in elevation since that time. Subsequent studies by Horton et al. (2004) and by Horton and Chamberlain (2006) that exploited other minerals and a longer duration of geologic time reached the same conclusion. None of these studies, however, included measurements from lowland California. Because of likely climate change since Miocene and early Pliocene time, and highly variable climate beginning in late Pliocene time, the similarity between modern and ancient  $\delta^{18}\text{O}$  values could reflect a combination of changes in elevation and climate. More important, as all of Poage and Chamberlain (2002), Horton et al. (2004), and Horton and Chamberlain (2006) recognized, precipitation falling in the Basin and Range Province derives largely from the tropical Pacific and does not pass over the Sierra Nevada (Friedman et al., 2002a, 2002b). Thus as interesting and stimulating as their work is, it may not bear on the question of when the Sierra Nevada rose to its present elevation.

More recently, Mulch et al. (2008) contrasted deuterium isotopes in middle Miocene to late Pleistocene volcanic glass from sites in the Great Valley of California, west of the Sierra Nevada, with those from sites in the Basin and Range Province ~300 km to the east (Fig. 1). Deuterium isotopes in volcanic glass, like those in modern clays, are systematically offset from those in precipitation because of fractionation of hydrogen isotopes during their incorporation into the clay minerals. When such fractionation is taken into account (Friedman et al. 1993), reconstructed deuterium concentrations of volcanic glasses match closely those calculated for modern precipitation in the same areas (Figs. 1 and 2). Assuming that the isotopic differences result from depletion of deuterium from vapor during orographic precipitation, Mulch et al. (2008) interpreted the large difference in deuterium isotope concentrations from the two regions in terms of an essentially constant elevation of the highest barrier to eastward flow, which they associated with the crest of the Sierra, from middle Miocene to present time.

Crowley et al. (2008) carried out a similar analysis of oxygen isotopes in tooth enamel from Miocene to modern mammal fossils (Fig. 1). They too allowed for fractionation of  $^{18}\text{O}$  as it is incorporated into tooth enamel, and they showed that in most time intervals since early Miocene time, the difference in  $\delta^{18}\text{O}$  values from fossil tooth enamel east and west of the Sierra Nevada was ~6‰, the present-day difference in precipitation across the range. (Temporal resolution of fossil teeth was too coarse for them to address the past 2 Myr.) Cautiously, they too attributed the similarity between past and present-day dif-

**Figure 1.** Map of a part of western North America showing the locations of the Sierra Nevada, Basin and Range Province, regions where Cassel et al. (2009) and Mulch et al. (2006) worked, and subsets of sample sites of Crowley et al. (2008) and Mulch et al. (2008).

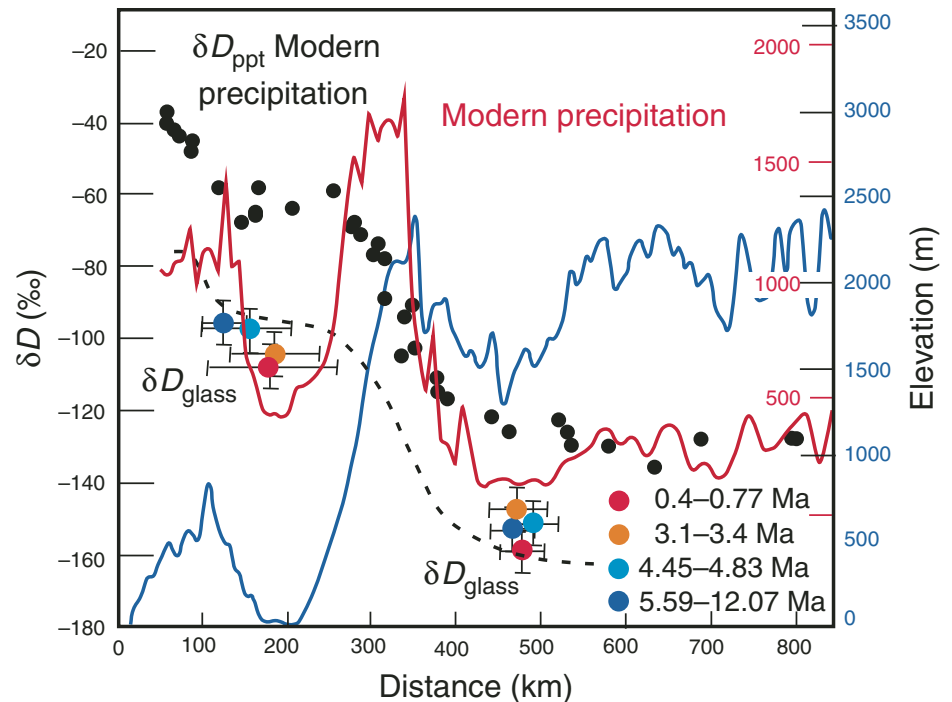
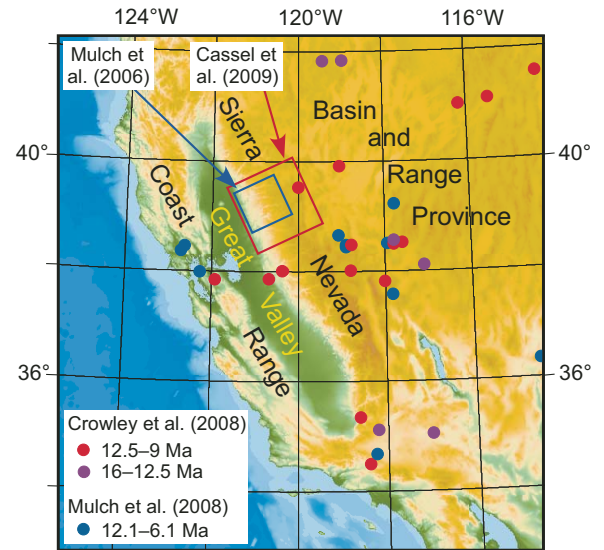


**Figure 2.** Topography (blue), modern precipitation in mm/yr (red), and deuterium isotopic ratios of modern precipitation (black circles: from Ingraham and Taylor, 1991) and in volcanic glass (blue, cyan, orange, and red circles with error bars) across the California and Nevada (Mulch et al., 2008). The dashed black line shows the deuterium isotopic ratios in glass for modern precipitation, calculated using the hydrogen glass–water fractionation factor from Friedman et al. (1993). Rainout on the windward side of the Sierra Nevada leads to a decrease in  $\delta D_{\text{precipitation}}$  of ~50‰. (Redrawn from figures in Mulch et al., 2008.)

ferences in  $\delta^{18}\text{O}$  values to a past elevation distribution similar to that at present.

Earlier, Mulch et al. (2006) reported deuterium concentrations in kaolinite that formed in situ in Eocene sediment deposited in the

paleo-Yuba River in the Sierra Nevada (Figs. 1 and 3). They showed that deuterium isotopes from the sediment decrease eastward across the Sierra Nevada with a gradient similar to that in modern precipitation but offset again because

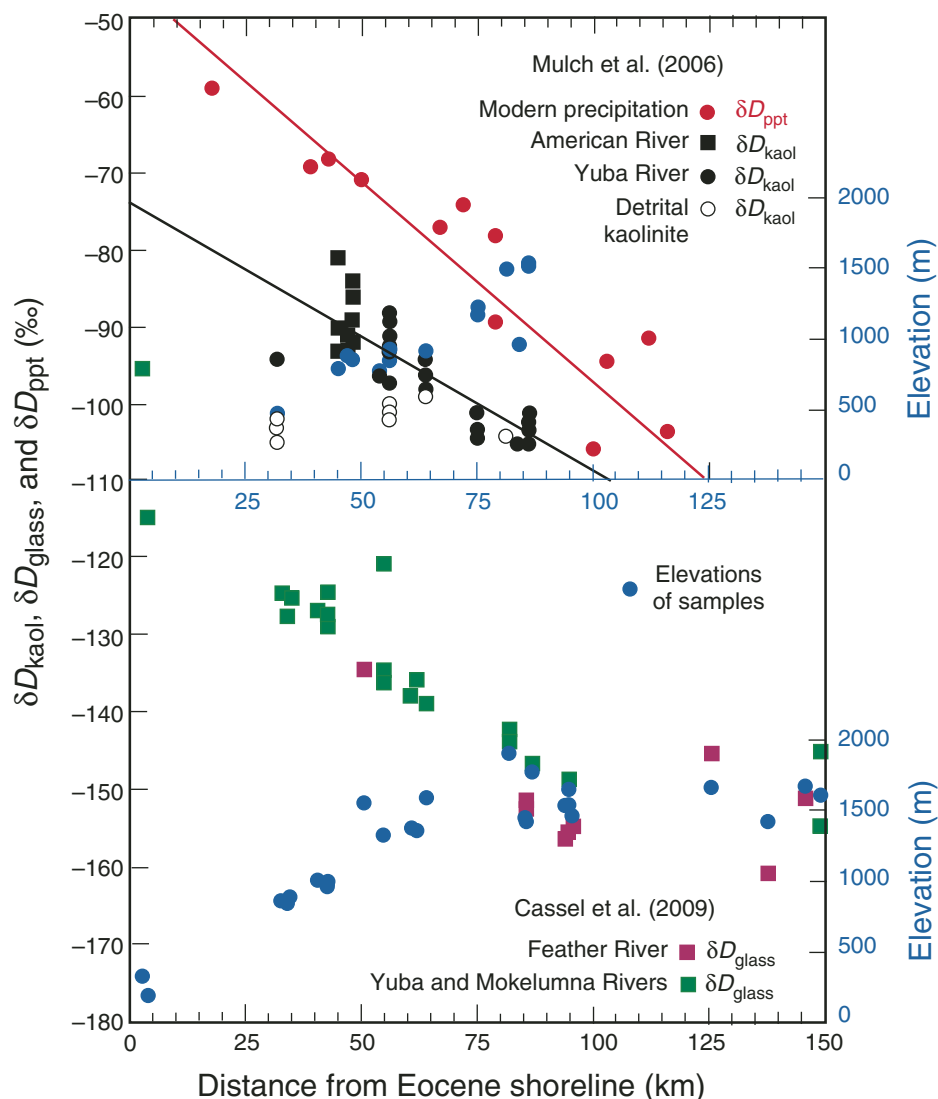


**Figure 3.** Profiles of deuterium isotope ratios as a function of distance from the Eocene shoreline, according to Dickinson et al. (1979). **Top:** Eocene deuterium isotope ratios for kaolinite,  $\delta D_{\text{kaol}}$  (black circles and squares) and for modern precipitation,  $\delta D_{\text{ppt}}$  (red circles), and elevations (blue circles) where Mulch et al. (2006) measured  $\delta D_{\text{kaol}}$  values. Black circles and squares show  $\delta D_{\text{kaol}}$  from kaolinite formed in situ from the Yuba and American Rivers, and open circles show  $\delta D_{\text{kaol}}$  detrital kaolinite along the Yuba River. The black line is a fit to  $\delta D_{\text{kaol}}$  from kaolinite formed in situ versus distance; the red line is the slope that Mulch et al. (2006) show for  $\delta D_{\text{ppt}}$  versus distance. **Bottom:** Oligocene deuterium isotope ratios for volcanic glass,  $\delta D_{\text{glass}}$  (green and purple squares for different river valleys), and elevations (blue circles) where Cassel et al. (2009) measured  $\delta D_{\text{glass}}$ .

of fractionation during incorporation in the kaolinite. More recently, Cassel et al. (2009) presented a similar analysis for deuterium in volcanic glass dated at 31–28 Ma, and they too showed an eastward decrease across the Sierra Nevada into the Basin and Range Province (Figs. 1 and 3). From these similarities, Mulch et al. (2006) and Cassel et al. (2009) suggested that the Eocene and Oligocene regional slopes

of the Sierra Nevada were indistinguishable from that today.

All of the authors noted above assumed that the same processes of orographically enhanced precipitation and fractionation of heavy isotopes occurred earlier in Cenozoic time as they do today, and all recognized limitations of that assumption. My purpose here is not to challenge their data or their other basic assump-

tions, but to offer an alternative to their tectonic interpretations and to suggest that the data of Cassel et al. (2009), Crowley et al. (2008), Horton and Chamberlain (2006), Horton et al. (2004), Mulch et al. (2006, 2008), and Poage and Chamberlain (2002) permit a late Miocene–Early Pliocene tilting of the Sierra Nevada.

## OROGRAPHIC PRECIPITATION

Although thermodynamics enters each stage that takes deuterium or  $^{18}\text{O}$  from vapor to kaolinite, volcanic glass, or tooth enamel, the dominant process that depends on elevation occurs during condensation from vapor to liquid phase, which precipitation then transports to Earth's surface. Thus, like all of Cassel et al. (2009), Crowley et al. (2008), Horton and Chamberlain (2006), Horton et al. (2004), Mulch et al. (2006, 2008), and Poage and Chamberlain (2002), I treat the deuterium and oxygen isotopes as a measure of the precipitation history that an air mass undergoes as it moves upward and over high terrain.

### The Simple Upslope Model

In the simplest model of orographic precipitation, as air moves horizontally and then up the slope of a mountain range, it eventually cools sufficiently that vapor condenses and then precipitates. The condensation rate, or the rate (per unit area per unit time) that vapor converts to cloud water, is assumed to be given by  $S(x, z) = \rho q_v w$ , where  $\rho$  is the density of air,  $q_v$  is the specific humidity (ratio of vapor to dry air plus vapor) at the surface, and  $w$  is the rate that air rises (Table 1 lists symbols and gives typical values of the quantities that they represent). For air moving up a slope, this becomes the “simple upslope model” (e.g., Roe, 2005; Smith, 1979):

$$S(x, z) = \rho q_v U \frac{dh}{dx}. \quad (1)$$

Here  $U$  is the wind speed during rain events (not prevailing westerly wind speeds, or speeds of mid-latitude jets), and  $dh/dx$  is the slope of the terrain with height  $h(x)$ . Most (e.g., Roe, 2005; Roe and Baker, 2006; Smith and Barstad, 2004) presume that cloud water precipitates after some relatively short interval of time,  $\tau_c \sim 1000$  s, but this delay is commonly ignored in the simple upslope model, if Smith (2003) did address its effects. Thus, eq. (1) gives an indication of how precipitation might vary across a mountain range.

The specific humidity  $q_v$  depends strongly on temperature. We may write  $q_v = RH q_v^*$ , where  $RH$  is relative humidity, and  $q_v^*$  is the saturation specific humidity (the fraction of water vapor in the air):

TABLE 1. LIST OF SYMBOLS AND TYPICAL VALUES

| Symbol                            | Typical value                                              | Meaning and, where appropriate, defining equation                                |
|-----------------------------------|------------------------------------------------------------|----------------------------------------------------------------------------------|
| $a$                               | 30 km                                                      | Scaling horizontal dimension for rise onto plateau (A2)                          |
| $e_{v0}$                          | 611 Pa                                                     | Saturated vapor pressure (2)                                                     |
| $h$                               | <4 km                                                      | Surface elevation (1)                                                            |
| $p$                               | 101 kPa                                                    | Sea level pressure (2)                                                           |
| $q_v$                             | 0.001–0.02                                                 | Specific humidity (1)                                                            |
| $q_0$                             | 0.001–0.02                                                 | Specific humidity at the surface (B2)                                            |
| $q_v^*$                           | 0.001–0.02                                                 | Saturation specific humidity (2)                                                 |
| $v_f$                             | 4 m s <sup>-1</sup>                                        | Fall speed of rain drops (B2)                                                    |
| $w$                               |                                                            | Vertical component of velocity of air                                            |
| $x$                               |                                                            | Horizontal position                                                              |
| $z$                               |                                                            | Vertical position                                                                |
| $C_w$                             | 0.001–0.02 kg m <sup>-3</sup>                              | Climate sensitivity factor (A5)                                                  |
| $H$                               | 2–4 km                                                     | Maximum height of ridge, mountain range, or plateau (A2, B1)                     |
| $H'$                              | 0.5–2                                                      | Normalized moisture scale height (A6)                                            |
| $H_w$                             | 2–4 km                                                     | Moisture scale height (A1)                                                       |
| $L$                               | 2.5 × 10 <sup>6</sup> J kg <sup>-1</sup>                   | Latent heat of vaporization (2)                                                  |
| $N$                               | 0.005–0.01 s <sup>-1</sup>                                 | Brunt-Väisälä frequency (A7)                                                     |
| $P$                               | 1–20 × 10 <sup>-4</sup> kg m <sup>-2</sup> s <sup>-1</sup> | Precipitation rate (per unit area per unit time)                                 |
| $R$                               | 287 J K <sup>-1</sup> kg <sup>-1</sup>                     | Gas constant for dry air (2)                                                     |
| $R_v$                             | 461 J K <sup>-1</sup> kg <sup>-1</sup>                     | Gas constant for vapor (2)                                                       |
| $RH$                              | 0.75                                                       | Relative humidity                                                                |
| $T$                               | 200–300 K                                                  | Temperature in the atmosphere (2)                                                |
| $T_s$                             | 270–300 K                                                  | Surface temperature (A1)                                                         |
| $U$                               | 10 m/s                                                     | Wind speed, during rain storms (1)                                               |
| $W$                               | 100 km                                                     | Width of upslope side of mountain range (B1)                                     |
| $\delta D_{\text{glass}}$         | –90 to –160‰                                               | Deuterium isotope values from volcanic glass                                     |
| $\delta D_{\text{kaol}}$          | –80 to –140‰                                               | Deuterium isotope values from kaolinite                                          |
| $\delta D_{\text{ppt}}$           | –40 to –140‰                                               | Deuterium isotope values from modern precipitation                               |
| $\gamma$                          | –7 to –1 K km <sup>-1</sup>                                | Lapse rate (A1)                                                                  |
| $\rho$                            | 1.2 kg m <sup>-3</sup>                                     | Density of air at the surface (1)                                                |
| $\rho_s$                          | 0.001–0.02 kg m <sup>-3</sup>                              | Water vapor density (A5)                                                         |
| $\tau_c$                          | 200–2000 s                                                 | Precipitation delay time (B2)                                                    |
| $\tau_{ev}$                       | 200–2000 s                                                 | Evaporation delay time                                                           |
| $\Gamma_m$                        | –9 to –5 K km <sup>-1</sup>                                | Moist adiabatic lapse rate (A7)                                                  |
| $\Delta C$                        | 10–1000 kg m <sup>-1</sup> s <sup>-1</sup>                 | Rainout: precipitation per unit length per unit time (A8)                        |
| $\Delta P$                        | 10–1000 kg m <sup>-1</sup> s <sup>-1</sup>                 | Rainout: precipitation per unit length per unit time (3, 4)                      |
| $\Delta(\delta D_{\text{glass}})$ | 50‰                                                        | Difference in $\delta D_{\text{glass}}$ between Great Valley and Basin and Range |
| $\Delta(\delta D_{\text{ppt}})$   | 65‰                                                        | Difference in $\delta D_{\text{ppt}}$ between Great Valley and Basin and Range   |

$$q_v^* \approx \frac{R}{R_v} \frac{e_{v0}}{p} \exp \left[ \frac{L}{R_v} \left( \frac{1}{273} - \frac{1}{T} \right) \right]. \quad (2)$$

$R$  (= 287 J K<sup>-1</sup> kg<sup>-1</sup>) and  $R_v$  (= 461 J K<sup>-1</sup> kg<sup>-1</sup>) are the gas constants for dry air and vapor,  $e_{v0}$  (= 611 Pa) the saturation vapor pressure at 273 K,  $p$  (= 101 kPa) is standard sea level pressure,  $L$  (= 2.5 × 10<sup>6</sup> J kg<sup>-1</sup>) is the latent heat of vaporization, and  $T$  is temperature in kelvins. For sensible surface temperatures,  $q_v^*$  increases by ~7%/°C temperature increase (e.g., Allan and Soden, 2008).

Regarding the decreasing  $\delta D_{\text{kaol}}$  values in Eocene stream gravel in the Sierra (Mulch et al., 2006) and the decreasing  $\delta D_{\text{glass}}$  values in the Oligocene volcanic glass (Cassel et al., 2009) (Fig. 3), suppose that the Eocene and Oligocene slopes of the Sierra Nevada were half that today. For a profile of eastward decreasing values to resemble that in modern precipitation, and hence with the assumption that moisture moves from west to east as most of it does for the Sierra Nevada today (e.g., Friedman et al., 2002b), the simple upslope model implies that to counteract a halving of  $dz/dx$ , the product  $\rho q_v U$  must have been two times larger. Relegating discussion of how wind speed,  $U$ , might have differed

in Eocene or Oligocene time to a section below, and recognizing that the density of air would not have changed significantly, a larger value of  $q_v$  does seem more likely for the Eocene and Oligocene epochs than for today.

Estimates of mean annual surface temperatures of 18–23 °C in the Puget Sound area in Eocene time (50–43 Ma) based on leaf physiognomy (Wolfe et al., 1998) suggest that that region was warmer by ~7–12 °C than its present-day mean annual temperature of 11 °C, despite that region having been several degrees farther north. Assuming the same relative humidity as today, a reasonable assumption for coastal environments, then from eq. (2), if the air crossing the Eocene shoreline of California were 7–12 °C warmer than today,  $q_v$  would have been greater than today by 1.6–2.2 times. It seems unlikely that Eocene temperatures in coastal California were 12 °C higher than today, but a difference of 7 °C lies within the plausible range (Zachos et al., 1994). Thus, greater warmth in Eocene time means that air could carry more moisture than today, and therefore offers an alternative to the inference that tilt of the Sierran block has been minimal since Eocene time.

The samples studied by Cassel et al. (2009) date from 31 to 28 Ma, after an ice sheet formed on Antarctica (e.g., Coxall et al., 2005; Zachos et al., 2001), when global climate presumably cooled, and when inland Asian climate became more arid (Dupont-Nivet et al., 2007). The proximity of the Sierra Nevada to the Pacific Ocean makes it unlikely that that area became more arid when ice formed on Antarctica, but the temperature difference between Oligocene and the present surely was smaller than that between Eocene and present time. Thus, a warmer Oligocene climate with more moisture than today will allow for a gentler gradient of the Sierra Nevada than that today, but alone it would not compensate for a gradient half that at present.

At present, most of the precipitation falling on the Sierra Nevada and in the Basin and Range Province falls in winter, when stable isotopes are more depleted than in summer (e.g., Friedman et al., 2002b). More relevant here, however, the specific humidity also is lower in winter than summer, as seasonal values obey eq. (2) reasonably well (Gaffen and Ross, 1999). Axelrod (1973) inferred from paleobotanical assemblages in southern California that the present-day Mediterranean climate, with dominantly winter precipitation, developed in middle Pliocene time. When Axelrod (1973) wrote this, middle Pliocene could have been as old as 6–8 Ma, and thus his timing cannot be applied with confidence, but more recent syntheses by Graham (1999, p. 254) and by Minnich (2007) suggests a change since ca. 5 Ma, if not more recent when upwelling of cool water along the California coastal current seems to have begun (Dekens et al., 2007). In any case, a switch from largely summer to largely winter precipitation could affect east-west profiles of stable isotopes.

If we consider the difference in stable isotopes between sites in the Great Valley and in the Basin and Range Province (Figs. 1 and 2), then to a first approximation, that difference would scale simply with the integrated difference in cloud water, or in rainout, at the two different heights. As the moist air moves up the slope of a mountain and loses moisture, condensation and precipitation deplete the vapor of deuterium. In the simple upslope model, the rate (per unit time, per unit distance perpendicular to the path of the air mass) at which vapor is lost to cloud water and then to precipitation is given by the integral over distance of eq. (1) to the point of interest,  $x = x_0$ :

$$\Delta P = \int_0^{x_0} S(x, z) dx = \rho q_v U h(x = x_0). \quad (3)$$

Thus, the slope ceases to be important; only the difference in heights affects the depletion of deuterium in air.

Mulch et al. (2008) reported similar values of differences between modern  $\delta D_{\text{ppt}}$  and of past (0.6–12 Ma)  $\delta D_{\text{glass}}$  at sites west and east of the Sierra Nevada,  $\Delta(\delta D_{\text{ppt}})$  and  $\Delta(\delta D_{\text{glass}})$  (Fig. 2). Crowley et al. (2008) noted similar differences for  $\delta^{18}\text{O}$  in modern precipitation and in fossil mammal tooth enamel. With explicit caution, both suggested that the same rain shadow present today and associated with the Sierra Nevada existed at these earlier times, but other ranges farther east could also contribute to that rain shadow. Paleoelevations of the sites in the Basin and Range differed little from those today, as leaf physiognomy from many of these basins shows (Wolfe et al., 1997). The simple upslope model (1) predicts the same rainout (3) for a path from sea level to present elevations, regardless of where high terrain lies, and hence its application to sites throughout much of the Basin and Range Province neither requires nor disallows a past elevation of the Sierra Nevada similar to that of today.

Some of the samples used by Mulch et al. (2008), however, come from the eastern margin of the Sierra Nevada, and an application of the upslope model to these  $\delta D_{\text{glass}}$  values with the same specific humidity would yield the same conclusion that they reached: the height of the Sierra Nevada since middle Miocene time need not have changed. Again, however, either a somewhat warmer Miocene climate or greater summer than winter precipitation, as Axelrod (1973), Graham (1999), and Minnich (2007) inferred, could compensate for a lower crest of the Sierra Nevada.

Also  $\delta D_{\text{glass}}$  values of Mulch et al. (2008) west of the Sierra fall 5–10‰ below those predicted by assuming present-day precipitation and a constant fractionation between water and glass (Fig. 1), and those east of the Sierra fall 5–10‰ above the line. Thus, whereas the difference in  $\delta D_{\text{ppt}}$  between sites in the Basin and Range Province and the Great Valley is ~65‰,  $\delta D_{\text{glass}}$  differs by only ~50‰. Mulch et al. (2008) recognized that the 15‰ increase in the difference between Miocene and Pliocene  $\delta D_{\text{glass}}$  and present-day  $\delta D_{\text{ppt}}$  might be taken to imply that the Miocene height of the rain shadow, at the Sierran crest or farther east, was lower by a small amount, ~500 m, than today.

The simple upslope model omits many processes, and it fails in obvious details. Smith et al. (2003, 2005) pointed out that it tends to overestimate precipitation during major rainstorms. It does not take into account the evaporation of raindrops before they hit the ground, or dynamics in the atmosphere that are stimulated by flow over terrain and that affect precipitation. Nevertheless, it allows an assessment of

potentially relevant elements, and more importantly, it forms the core of more complicated, more realistic models.

### Smith and Barstad's (2004) Model of Orographic Precipitation

Smith and Barstad (2004) extended the simple upslope model by allowing for dynamic processes in the atmosphere and for a finite height above Earth's surface in which water vapor is significant. As an air mass impinges on topography, the back pressure imposed by the topography disrupts the static state of an atmospheric column. In a stably stratified atmosphere, this pressure generates standing gravity waves that attenuate upward and into the wind. Thus, the air mass becomes sensitive to the topography before it passes over it. The thicker the layer of moisture, the more vapor that a column of the atmosphere contains. Whereas on the one hand, a deeper moist layer might produce more precipitation, on the other, much of the vapor is high enough that it is only mildly sensitive to the topography below. Air even only a few thousand meters aloft moves gradually upward along a path not equidistant from the topography, and its vapor need not cool sufficiently to condense.

Among idealized topographic profiles that they considered, Smith and Barstad (2004) derived an analytical solution for the rate of cloud formation over a simple, gradual step from a lowland onto a plateau whose topographic profile is given by eq. (A2). They obtained a cloud formation rate (per unit area per unit time) for an air mass flowing up such topography that is given by eq. (A4). As discussed in Appendix A, the cloud formation rate, and hence the precipitation rate, consists essentially of the simple upslope model modified by a factor that depends on the decrease of moisture with elevation. This factor also depends on the static stability of the atmosphere, the degree to which an air mass that is perturbed upward or downward returns to its initial elevation, and on the wind speed  $U$ .

Allowing for a finite thickness of moisture and a finite static stability spreads the locus of cloud formation and shifts its maximum upwind, via the term in the numerator of eq. (A4) (Fig. A1). This is an obvious virtue of the model, because rainfall commonly is heavy at the foot of the windward side of a mountain range (west coast of New Zealand, for example). Compared with the simple upslope mode, the precipitation rate is smaller, because air aloft is less sensitive to the topography than the air just above the surface, which is quantified by the denominator in eq. (A4). Consequently, less of the moisture in a deep moist layer condenses than when a thinner basal layer follows

the same topography, and vertical displacements of vapor are large (Fig. A1).

The similarity of Smith and Barstad's (2004) linear model to the simple upslope model concurs with the inferences given above: that the Eocene and Oligocene gradients in  $\delta D_{\text{kaol}}$  and  $\delta^{18}\text{O}$  (Fig. 3) do not require similar Eocene, Oligocene, and present-day slopes of the Sierra Nevada.

In converting the cloud formation rate to precipitation, Smith and Barstad (2004) also allowed for a finite delay,  $\tau_c$ , for cloud water to begin to precipitate. Then, to test the model with observed precipitation, Barstad and Smith (2005) and Smith et al. (2005) focused mostly on individual storms, and their tests to some extent represent efforts to find best fitting values of  $\tau_c$ . Perhaps most interesting for a discussion of the Sierra Nevada is the observation by Smith et al. (2005) that the model works better on small distance scales (<10 km) than on larger ones. Part of the limitation might be that the cloud time delay,  $\tau_c$ , is not a constant, independent of region or storm. Although all values of  $\tau_c$  lie within the range of 600–2400 s, more physics than Smith and Barstad (2004) included must affect this quantity. Moreover, the regions that they considered tend to be characterized by chains, such as the Wasatch Range, Utah, and the Lago Maggiori area on the southern edge of the Alps (Barstad and Smith, 2005) or the Cascades (Smith et al., 2005), that are narrower than the Sierra Nevada. Thus, if better than the simple upslope model, Smith and Barstad's (2004) linear model also is imperfect in ways that limit its applicability to the Sierra Nevada. Nevertheless, it shows essentially the same dependence on elevation as the simple upslope model, and if applied to the Sierra Nevada, it would allow the same tradeoffs between elevations and specific humidity.

### Roe and Baker's (2006) Model of Orographic Precipitation

Roe and Baker (2006) took a different approach to estimating orographic precipitation, which they based largely on simple kinematics of an air mass impinging on a ridge. They too assumed that vapor decreases exponentially upward with a moisture scale height  $H_w$ , as in eq. (A1), and that it condenses as air ramps upward above sloping topography. The condensate then is assumed to precipitate after a cloud time delay,  $\tau_c$ , as Smith and Barstad (2004) assumed. Once converted to precipitation, rain falls with a terminal speed  $v_f$  (~4 m/s) as it is carried downwind. This model has the weakness that no precipitation falls over the base of the upwind slope. Orographic precipitation begins at a

distance given by  $U\tau_c$  (~10 km for typical values of  $U = 10$  m/s and  $\tau_c = 1000$  s) downwind of the base of the mountain front (Fig. B1).

For a sloping surface of maximum height  $H$  and width  $W$ , Roe and Baker (2006) derived an expression for precipitation on the windward slope that once again resembles the simple upslope model (see Appendix B, equation B2 or B3). The factors of the upslope model in eq. (3) are modified by another factor that allows for precipitation to fall from a range of heights with a terminal speed. The calculated precipitation begins when the air has risen sufficiently high to condense, and then rises rapidly with downwind distance toward the mountain range before decaying exponentially, as moisture is wrung out of the atmosphere (Fig. B1). Thus, like Smith and Barstad's (2004) model, with more adjustable parameters than the simple upslope model, it too can account for the similar gradients of Eocene  $\delta D_{\text{kaol}}$  or  $\delta D_{\text{glass}}$  and  $\delta D_{\text{ppt}}$  in modern precipitation (Fig. 2).

Again, as with eqs. (3) and (A8), the total depletion of moisture by precipitation falling on the windward slope is independent of the slope or the width of the range. With the same order of simplifications as in Appendix B, depletion of moisture is

$$\Delta P = \int_{-w}^0 P(x) dx \approx \rho q_v U H_w \left[ 1 - \exp\left(-\frac{H}{H_w}\right) \right]. \quad (4)$$

If the height of the range is much smaller than the moisture scale height,  $H \ll H_w$ , this reduces exactly to the simple upslope model. In the opposite extreme limit of a very high range,  $H \gg H_w$ , all moisture precipitates before the air mass crosses the summit of the range. For a point east of the crest ( $x = 0$ ), Roe and Baker's (2006) calculated orographic precipitation on the leeward side of the range is small (see Appendix B, Fig. B1).

Thus, once again, the similar differences in stable isotopes on the leeward and windward sides of the Sierra Nevada for geologic materials and for modern precipitation can allow for a lower crest of the Sierra Nevada in warmer climate, especially if dominated by summer precipitation.

### Wind Speed, $U$

As most readers must have noticed, by assigning a value of  $U = 10$  m/s, I have ignored a quantity that might undermine, if not negate, all claims made above about the height or slope of the Sierra Nevada, or might, conceivably, strengthen the arguments given above. Alas, the wind speed as used here risks sharing qualities with a "can of worms," "Pandora's box," or

whatever simile one might use to render elegant quantitative arguments only qualitative at best.

The wind speed used here is not the mean annual, or even monthly average, wind speed, but is the wind speed that characterizes a rainy period. Thus, how it might depend on climate is hardly obvious. There is little to show that wind speeds near the surface during rainstorms should have been lower (or higher) in earlier Cenozoic time than at present. Using regional climate model calculations, Frei et al. (1998) showed that precipitation increases with increased specific humidity, according to eq. (2), but they did not discuss winds or orographic precipitation specifically.

There is sensible reason to suspect that winds aloft at temperate latitudes are higher today than they were in Eocene, Oligocene, or middle Miocene time. The atmosphere maintains a quasi-steady state, in which thermal wind balance applies: the vertical gradient in westerly wind speed is proportional to the meridional surface temperature gradient. The meridional temperature gradient in Eocene time was roughly half that today (Zachos et al., 1994), and thus the jet speed at the top of the troposphere in mid-latitudes (height of ~12 km) could have been roughly half that today. As noted above, however, that wind speed is not what enters the theories of orographic precipitation. Moreover, Roe and Baker (2006), as well as Colle (2004) using a more realistic mode, showed that greater wind shear reduces their calculated orographic precipitation. Adding a wind shear of  $0.003 \text{ s}^{-1}$  (as one might expect from a speed of ~30 m/s at a height of 10 km) reduces Roe and Baker's (2006) calculated orographic precipitation by ~25%. For a wind shear of  $0.0015 \text{ s}^{-1}$ , the reduction is closer to 15%. Thus, although negligibly small compared to uncertainties in assumed parameters (and other assumptions), the stronger present-day wind shear might reduce, as well as redistribute, orographic precipitation compared to that in earlier times.

### More Realistic Models of Orographic Precipitation

The three simple models discussed above ignore numerous aspects of atmospheric dynamics and thermodynamics (such as phase changes between ice and liquid water) that might make them inappropriate for comparison with real data. Indeed, a rich literature shows that most complexities ignored here affect the distribution and amounts of precipitation, and to simulate individual rainstorms usefully, such complexities must be included. When one considers multi-year average conditions, however, complexities that affect individual rainstorms will to some ex-

tent cancel one another when numerous storms with different dynamic and thermodynamic conditions apply to each.

One obvious oversimplification is the assumed two-dimensional structure of both the mountain range and the atmospheric circulation. Galewsky (2008, 2009a, 2009b) has shown that for mountains as high as the Sierra Nevada, wind speeds must exceed 10 m/s for flow to pass over the crest of a range of the dimensions of the Sierra Nevada rather than around the northern or southern ends of the range. Thus, he contested the most basic assumption assumed both here and in the analyses of stable isotopes discussed above, that precipitation and hence stable isotopes depend on the maximum height of the topography (Galewski, 2009a, 2009b). Accordingly, he too questioned inferences of Sierra paleoaltimetry based on stable isotopes.

### CONCLUSIONS

Measurements of stable isotope concentrations in a variety of geological materials east and west of the Sierra Nevada and within the belt reveal east-west gradients or differences that resemble those in modern isotopic concentrations of modern-day precipitation (e.g., Cassel et al., 2009; Crowley et al., 2008; Mulch et al., 2006, 2008). Recognizing that during condensation, heavy isotopes such as deuterium preferentially move from vapor to liquid phase, and that orography plays a primary role in such condensation and precipitation, these authors, as well as others with slightly different distributions of samples (Horton and Chamberlain, 2006; Horton et al., 2004; Poage and Chamberlain, 2002), suggested that the similarities between modern and geological isotopic concentrations imply that the orography of the Sierra Nevada has changed little during most of Cenozoic time. This inference, however, contradicts interpretations of geomorphic observations from the Sierra in which the entire Sierra Nevada tilted about an axis parallel to and along its base in late Miocene or early Pliocene time, and that the crest of the Sierra has risen 1000–2000 m since that time (e.g., Christensen, 1966; Huber, 1981, 1990; Jones et al., 2004; Lindgren, 1911; Stock et al., 2004, 2005; Unruh, 1991; Wakabayashi and Sawyer, 2001).

Using simple models for orographic precipitation (Roe, 2005; Roe and Baker, 2006; Smith, 1979; Smith and Barstad, 2004), I argue that the similarities of deuterium isotopes in Eocene kaolinites (Mulch et al., 2006) ( $\delta D_{\text{kaol}}$ ) and in Oligocene volcanic glasses (Cassel et al., 2009) to those in modern precipitation ( $\delta D_{\text{ppt}}$ ) across the Sierra Nevada do not require similar slopes for the Sierra Nevada. Rather, a combination

of warmer Eocene and Oligocene climates and a gentler slope of the Sierra could account for this similarity. I also consider the differences between  $\delta D$  values in Miocene to Pleistocene volcanic glasses from the Great Valley of California and from the Basin and Range Province in Nevada (Mulch et al., 2008) and between  $\delta^{18}O$  in tooth enamel from these two regions (Crowley et al., 2008). Both differences are similar to those in  $\delta D$  and  $\delta^{18}O$  values in modern precipitation at these localities. I argue that these similarities place only weak constraints on the history of the Sierra Nevada, again because a different climate could compensate for lower elevations. As elegant as the studies of Cassel et al. (2009), Crowley et al. (2008), and Mulch et al. (2006, 2008) are, nonuniqueness in the interpretation of orographic precipitation denies their isotopic measurements a robust constraint on hypothesized elevation histories of the Sierra Nevada.

ACKNOWLEDGMENTS

I have been stimulated by discussions with and encouragement from S.A. Graham, C.H. Jones, A. Mulch, and G.H. Roe, and constructive criticism of the manuscript from C.N. Garziona, M. Kennedy, R. Minnich, and A. Mulch. This research was supported by the National Science Foundation through grant EAR-0607831.

APPENDIX A. DISCUSSION OF DETAILS IN SMITH AND BARSTAD'S (2004) MODEL

To allow for a finite thickness of moist air, Smith and Barstad (2004) assumed that specific humidity decreases exponentially with height:  $q(z) = q_s \exp(-z/H_w)$ , in which the moisture scale height is

$$H_w = -\frac{R_s T_s^2}{L\gamma}, \tag{A1}$$

where  $T_s$  is the surface temperature in kelvins, and  $\gamma = dT/dz$  is the lapse rate (a negative quantity) of the environmental air. Typical values of  $H_w$  are ~2–3 km in temperate environments, but can be as much as 4 km in the moist tropics where the magnitude of  $\gamma$  can be small (e.g., Roe, 2006).

As an example, Smith and Barstad (2004) derived an analytical solution for the rate of cloud formation over topographic profile given by

$$h_s(x) = H \left[ \frac{1}{2} + \frac{\tan^{-1}(x/a)}{\pi} \right]. \tag{A2}$$

Here,  $H$  = the height of the plateau, and  $a$  scales the width of the step (Fig. A1). The surface slope is

$$\frac{dh}{dx} = \frac{aH}{\pi(a^2 + x^2)}, \tag{A3}$$

with a maximum slope of  $H/\pi a$  (if this were applied to the present-day Sierra Nevada, with  $H \sim 2.5$  km and a maximum slope of  $\sim 0.025$ ,  $a \sim 30$  km).

Smith and Barstad (2004) obtained for the cloud formation rate (per unit area per unit time) for an air mass flowing up such topography:

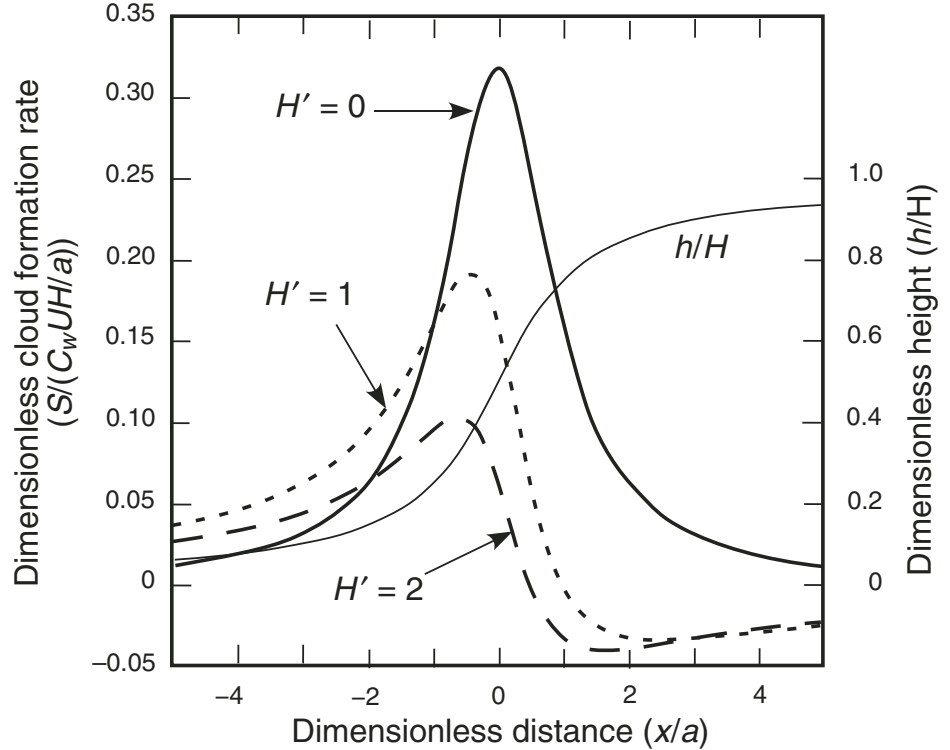


Figure A1. Dimensionless cloud formation rates calculated using Smith and Barstad's (2004) model, eq. (A4), for flow over a step in topography given by eq. (A2) and shown by the fine line. Solid, short-dashed, and long-dashed curves show the effect of increasing the normalized moisture scale height,  $H'$ , given by eq. (A6). Note that increasing  $H'$  both decreases precipitation and shifts its maximum downslope and toward the wind, as is clear in eq. (A4).

$$S(x) = C_w U \frac{dh(x)}{dx} \left[ \frac{1 - (x/a)H'}{1 + H'^2} \right]. \tag{A4}$$

Here the climate sensitivity factor,

$$C_w = \frac{\rho_s \Gamma_m}{\gamma}, \tag{A5}$$

is analogous to and within a factor of 2 of  $\rho q_s$ , in the simple upslope model (1), for  $\rho_s$  is the water vapor density ( $\rho q_s$ ) at the ground. The moist adiabatic lapse rate is  $\Gamma_m$  and depends on the surface temperature. The ratio of  $\Gamma_m/\gamma$  in  $C_w$  in eq. (A7) is close to unity. Thus, eq. (A4) describes the simple upslope model modified by a factor that depends on

$$H' = \frac{H_w N}{U}. \tag{A6}$$

$H'$  normalizes the moisture scale height and takes into account the stability of the atmosphere, which is parameterized by the Brunt-Väisälä frequency

$$N = \sqrt{-\frac{g}{\rho} \frac{d\rho}{dz}} = \sqrt{\frac{g(\gamma - \Gamma_m)}{T}}. \tag{A7}$$

Both  $\gamma$  and  $\Gamma_m$  are negative quantities, and obviously,  $\Gamma_m$  must be the larger in magnitude for  $N$  to be real, and for the atmosphere to be stable. For  $\Gamma_m$ , Smith and Barstad (2004) gave values of -9, -8, -7, -6, and -5 °C km<sup>-1</sup> for surface temperatures of 253, 263, 273, 283, and 293 K. For typical values of  $N \sim 0.005$ –

0.01 s<sup>-1</sup>,  $\gamma$  and  $\Gamma_m$  differ by ~0.8–3 °C/km, and thus  $0.5 < \Gamma_m/\gamma < 1$ . With typical values (Table 1, Appendix A) of  $H_w \sim 2$  km,  $N \sim 0.01$  s<sup>-1</sup>, and  $U \sim 10$  m/s,  $H' \sim 2$ .

Regarding the differences in stable isotopes between sites in the Great Valley and in the Basin and Range Province (Fig. 1), Smith and Barstad (2004) showed that the difference in cloud condensation rate between lowlands ( $x \leq -\infty$ ) and localities far onto the plateau ( $x \leq \infty$ ) is simply

$$\Delta C = \frac{C_w U H}{1 + H'^2}. \tag{A8}$$

Thus, the same argument given above, with its requisite strengths and weaknesses and shown by eq. (3), concerning the observations of Mulch et al. (2008) and Crowley et al. (2008) applies with a more realistic model for orographic precipitation: the similar differences between modern stable isotopes of precipitation and between those in geologic material at sites in the Basin and Range Province and in the Great Valley (Fig. 2), which presumably imply similar amounts of rainout of the air masses passing over the regions, allow for a lower Sierra Nevada than today.

APPENDIX B. DISCUSSION OF ROE AND BAKER'S (2006) MODEL AND SIMPLIFICATIONS TO IT

For a sloping surface of maximum height  $H$  and width  $W$  defined by:

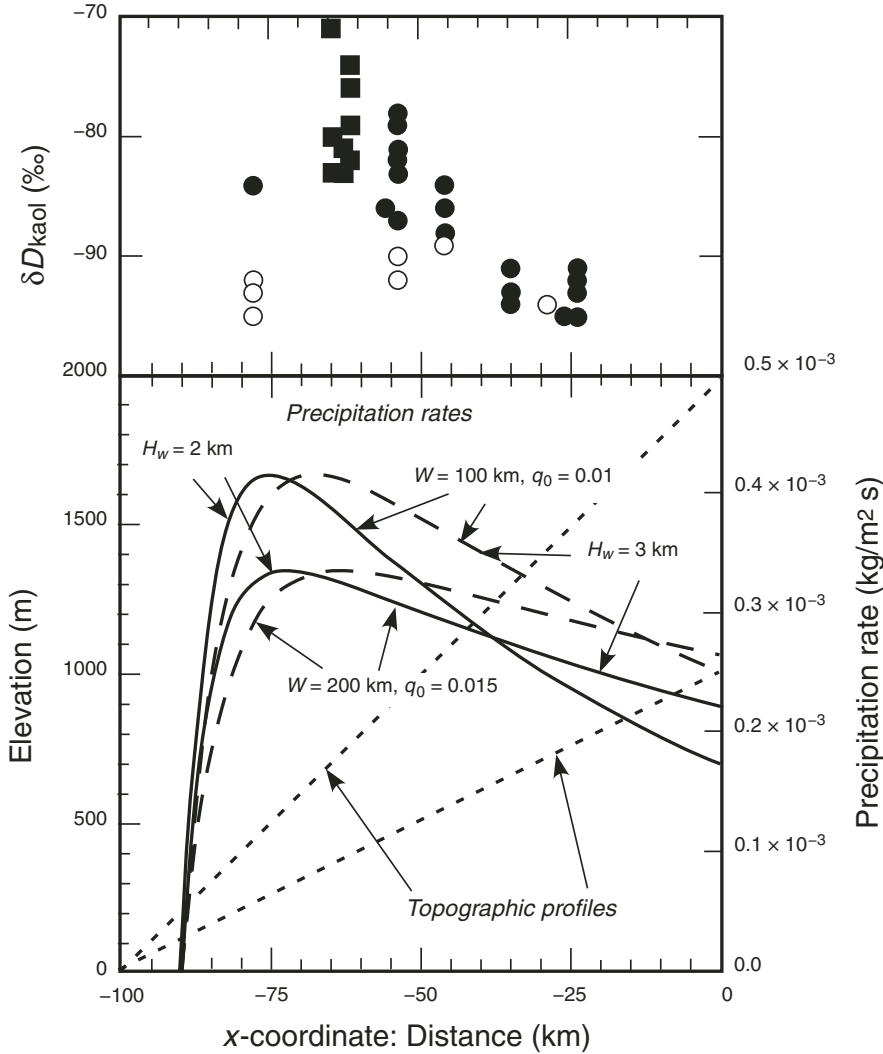


**Figure B1.** Dimensionless precipitation rates calculated using Roe and Baker's (2006) model, eqs. (B2) and (B9), for flow over a step in topography given by eq. (B1) and shown by the straight dashed lines. Different curves show the effects of different combinations of parameters on the calculated precipitation rates. In all calculations,  $\tau_{ec} = \tau_c$ . In the top plot, the deuterium isotopes from Mulch et al. (2006) in Figure 3 are replotted for comparison with precipitation rates in the lower plot.

$$h(x) = H \left( 1 + \frac{x}{W} \right), \text{ for } -W < x < 0, \quad (\text{B1})$$

Roe and Baker (2006) derived the following expression for precipitation on the windward slope:

$$P(x) = \frac{\rho q_0 U H}{W} F_1 \left[ F_2 \exp\left(-\frac{Hx}{WH_w}\right) - F_3 \exp\left(-\frac{v_f x}{UH_w}\right) \right], \quad (\text{B2})$$

where  $U\tau_c - W \leq x \leq 0$ ,  $F_1 = [Wv_f/(Wv_f - UH)]$ ,  $F_2 = \exp[H(U\tau_c - W/WH_w)]$ , and  $F_3 = \exp[v_f(U\tau_c - W/UH_w)]$ . The factor,  $F_1$ , accounts for the geometry of particle motion, the trajectory of raindrops to a sloping surface. The factors  $F_2$  and  $F_3$  result from a vertical integration through the moist atmospheric column whose different trajectories allow moisture to fall on the surface  $h(x)$  at position  $x$ . Only part of the atmospheric column can produce rainfall at any point;

air that is too low does not condense until passing that point, and condensate that forms too high will fall downwind of this point ( $x, h$ ). The differences between two terms in each exponential factor arise because of the height ranges over which precipitation falls.

Note that eq. (B2) can be approximated as

$$P(x) \approx \frac{\rho q_0 U H}{W} \left\{ \exp\left[-\frac{H}{H_w} \left(1 + \frac{x}{W}\right)\right] - \exp\left[-\frac{v_f W}{UH_w} \left(1 + \frac{x}{W}\right)\right] \right\}. \quad (\text{B3})$$

Substituting  $W \sim 100$  km and  $H \sim 2.5$  km, appropriate for the Sierra Nevada, and typical values such as  $U \sim 10$  m/s and  $v_f \sim 4$  m/s (Table 1) yields  $F_1 \approx 1$ . With  $\tau_c \sim 1000$  s and  $H_w = 2.5$  km,  $F_2 \approx \exp(-H/H_w) \sim e^{-1}$ .

For  $F_3$ , the second term in the exponent dominates, so that  $F_3 \approx \exp(-Wv_f/UH_w) \sim e^{-16}$ . The tiny value of this factor makes the second term appear to be negligibly small, but where  $x \sim -W$ , the second term is comparable to the first. Thus, eq. (B2) becomes eq. (B3).

An integration of the total precipitation falling on the windward side of a ridge yields

$$\begin{aligned} \Delta P &= \int_{-W+U\tau_c}^0 P(x) dx \\ &= \frac{\rho q_0 U H}{W} F_1 \left\{ \frac{WH_w}{H} \left[ 1 - \exp\left(\frac{HU\tau_c}{H_w W} - \frac{H}{H_w}\right) \right] - \frac{UH_w}{v_f} \left[ 1 - \exp\left(\frac{v_f \tau_c}{H_w} - \frac{Wv_f}{UH_w}\right) \right] \right\}. \quad (\text{B4}) \end{aligned}$$

Exploiting the values of parameters used above yields eq. (4).

For the leeward slope  $x \geq 0$ , Roe and Baker (2006) obtained an expression that can be simplified if the leeward side is a flat plateau, with no slope:

$$P(x) = \frac{\rho q_0 U H}{W} F_4 F_5 \exp\left[-\left(1 + \frac{v_f \tau_{ev}}{H_w}\right) \frac{x}{U\tau_{ev}}\right], \quad (\text{B5a})$$

where

$$F_4 = \exp\left[-\frac{H}{H_w} \left(1 - \frac{U\tau_c}{W}\right)\right] \exp\left[-\frac{Wv_f}{H_w U} \left(1 - \frac{U\tau_c}{W}\right)\right]. \quad (\text{B5b})$$

With the typical values of parameters assumed above,  $F_4 \approx 1$ . Roe and Baker (2006) assumed that the probability of evaporation increases exponentially with time during fall, which is a time constant  $\tau_{ev}$  as precipitation falls on the leeward side of the range. With typical parameters, including  $\tau_{ev} \sim 2000$  s, eq. (B5a) can be approximated by:

$$P(x) \approx \frac{\rho q_0 U H}{W} \exp\left(-\frac{H}{H_w}\right) \exp\left(-\frac{H_w + v_f \tau_{ev}}{U\tau_{ev} H_w} x\right). \quad (\text{B6})$$

The calculated rainout from  $x = 0$  to some distance into the plateau,  $x_0$ , is

$$\begin{aligned} \Delta P &= \int_0^{x_0} P(x) dx \approx \frac{\rho q_0 U H}{W} \frac{U\tau_{ev} H_w}{H_w + v_f \tau_{ev}} \exp\left(-\frac{H}{H_w}\right) \\ &\quad \times \left[ 1 - \exp\left(-\frac{H_w + v_f \tau_{ev}}{U\tau_{ev} H_w} x_0\right) \right]. \quad (\text{B7}) \end{aligned}$$

With the parameters used above, and with  $x_0 \sim 100$  km, the exponential term in brackets is negligible, and the second fraction in eq. (B7),  $U\tau_{ev} H_w / (H_w + v_f \tau_{ev}) \sim O(H_w)$ . Thus, rainout over the plateau in eq. (B7) would be only a few percent of that on the windward side, in eq. (B2).

The effects of different parameters on the precipitation rate can be seen best by rendering eqs. (B2) and (B5) dimensionless. With the following nondimensionalizations: distance,  $x' = x/W$ ; precipitation,  $P' = P(\rho q_0 U H/W)$ ; slope,  $s' = UH/Wv_f$ ; height,  $h' = H/H_w$ ; offset distance,  $x'_i = U\tau_c/W$ , eq. (B2) becomes:

$$\begin{aligned} P' &= \frac{1}{1-s'} \left[ \exp[h'(x'_i - x' - 1)] - \exp\left(\frac{h'x'_i - h'x' - 1}{s'}\right) \right], \quad (\text{B8}) \\ &\quad -x' \leq x' \leq 0. \end{aligned}$$

Then with a dimensionless evaporation decay distance,  $d'_{ev} = U\tau_{ev}/W$ , eq. (B5) becomes:

$$P' = \frac{1}{1-s'} \left\{ \exp[-h'(1-x'_i)] - \exp\left[-\frac{h'}{s'}(1-x')\right] \right\} \times \exp\left[-(1+h'd'_{ev})\frac{x'}{d'_{ev}}\right], \quad 0 \leq x'. \quad (\text{B9})$$

With typical values as in Table 1, the dimensionless quantities take on values like those given used for Figure B1, which shows the calculated dimensionless precipitation versus dimensionless distance for combinations of plausible parameters. The rapid rise in precipitation—slow decrease with distance, and then rapid drop when the plateau is reached—characterize all combinations.

## REFERENCES CITED

- Allan, R.P., and Soden, B.J., 2008, Atmospheric warming and the amplification of precipitation extremes: *Science*, v. 321, p. 1481–1484, doi: 10.1126/science.1160787.
- Axelrod, D.I., 1973, History of the Mediterranean Ecosystem in California, in di Castri, F., and Mooney, H.A., eds., *Ecological Studies: Analysis and Synthesis*, Volume 7: Berlin, Springer-Verlag, p. 225–277.
- Barstad, I., and Smith, R.B., 2005, Evaluations of an orographic precipitation model: *Journal of Hydro-meteorology*, v. 6, p. 85–99.
- Cassel, E.J., Graham, S.A., and Chamberlain, C.P., 2009, Cenozoic tectonic and topographic evolution of the northern Sierra Nevada, California, through stable isotope paleoaltimetry in volcanic glass: *Geology*, v. 37, p. 547–550, doi: 10.1130/G25572A.1.
- Chamberlain, C.P., and Poage, M.A., 2000, Reconstructing the paleotopography of mountain belts from the isotopic compositions of authigenic minerals: *Geology*, v. 28, p. 115–119, doi: 10.1130/0091-7613(2000)28<115:RTPOMB>2.0.CO;2.
- Christensen, M.N., 1966, Late Cenozoic crustal movements in the Sierra Nevada of California: *Geological Society of America Bulletin*, v. 77, p. 163–182, doi: 10.1130/0016-7606(1966)77[163:LCCMIT]2.0.CO;2.
- Colle, B.A., 2004, Sensitivity of orographic precipitation to changing ambient conditions and terrain geometries: An idealized modeling perspective: *Journal of Atmospheric Sciences*, v. 61, p. 588–606.
- Coxall, H.K., Wilson, P.A., Pälike, H., Lear, C.H., and Backman, J., 2005, Rapid stepwise onset of Antarctic glaciation and deeper calcite compensation in the Pacific Ocean: *Nature*, v. 433, p. 53–57, doi: 10.1038/nature03135.
- Crowley, B.E., Koch, P.L., and Davis, E.B., 2008, Stable isotope constraints on the elevation history of the Sierra Nevada Mountains, California: *Geological Society of America Bulletin*, v. 120, p. 588–598, doi: 10.1130/B26254.1.
- Dalrymple, G.B., 1963, Potassium-Argon dates of some Cenozoic rocks of the Sierra Nevada: *Geological Society of America Bulletin*, v. 74, p. 379–390, doi: 10.1130/0016-7606(1963)74[379:PDOSCV]2.0.CO;2.
- Dansgaard, W., 1964, Stable isotopes in precipitation: *Tellus*, v. 16, p. 436–467.
- Dekens, P.S., Ravelo, A.C., and McCarthy, M.D., 2007, Warm upwelling regions in the Pliocene warm period: *Paleoceanography*, v. 22, p. PA3211, doi: 10.1029/2006PA001394.
- Dickinson, W.R., Ingersoll, R.V., and Graham, S.A., 1979, Paleogene sediment dispersal and paleotectonics in northern California: *Geological Society of America Bulletin*, v. 90, Part II, p. 1458–1528.
- Dupont-Nivet, G., Krijgsman, W., Langerais, C.G., Abels, H.A., Dai, S., and Fang, X.-m., 2007, Tibetan plateau aridification linked to global cooling at the Eocene–Oligocene transition: *Nature*, v. 445, p. 635–638, doi: 10.1038/nature05516.
- Frei, C., Schär, C., Lüthi, D., and Davies, H.C., 1998, Heavy precipitation processes in a warmer climate: *Geophysical Research Letters*, v. 25, p. 1431–1434, doi: 10.1029/98GL51099.
- Friedman, I., and Smith, G.I., 1970, Deuterium content of snow cores from the Sierra Nevada area: *Science*, v. 169, p. 467–470, doi: 10.1126/science.169.3944.467.
- Friedman, I., Sheppard, R.A., and Gude, A.J., 1993, Deuterium fractionation as water diffuses into silicic volcanic ash, in *Climate Change in Continental Isotopic Records*: Washington, D.C., Geophysical Monograph, v. 78, American Geophysical Union, p. 321–323.
- Friedman, I., Harris, J.M., Smith, G.I., and Johnson, C.A., 2002a, Stable isotope composition of waters in the Great Basin, United States, 1: Air-mass trajectories: *Journal of Geophysical Research*, v. 107, no. D19, p. 4400, doi: 10.1029/2001JD000565.
- Friedman, I., Smith, G.I., Johnson, C.A., and Moscati, R.J., 2002b, Stable isotope composition of waters in the Great Basin, United States: 2. Modern precipitation: *Journal of Geophysical Research*, v. 107, no. D19, p. 4401, doi: 10.1029/2001JD000566.
- Gaffen, D.J., and Ross, R.J., 1999, Climatology and trends in U.S. surface humidity and temperature: *Journal of Climate*, v. 12, p. 811–828, doi: 10.1175/1520-0442(1999)012<0811:CATOUS>2.0.CO;2.
- Galewsky, J., 2008, Orographic clouds in terrain-blocked flows: An idealized modeling study: *Journal of the Atmospheric Sciences*, v. 65, p. 3460–3478, doi: 10.1175/2008JAS2435.1.
- Galewsky, J., 2009a, Rain shadow development during the growth of mountain ranges: An atmospheric dynamics perspective: *Journal of Geophysical Research*, v. 114, p. F01018, doi: 10.1029/2008JF001085.
- Galewsky, J., 2009b, Orographic precipitation isotopic ratios in stratified atmospheric flows: Implications for paleoelevation studies: *Geology*, v. 37, p. 791–794, doi: 10.1130/G30008A.1.
- Gat, J.R., 1996, Oxygen and hydrogen isotopes in the hydrologic cycle: *Annual Review of Earth and Planetary Sciences*, v. 24, p. 225–262, doi: 10.1146/annurev.earth.24.1.225.
- Graham, A., 1999, Late Cretaceous and Cenozoic History of North American Vegetation (North of Mexico): New York, Oxford University Press, 350 p.
- Horton, T.W., and Chamberlain, C.P., 2006, Stable isotopic evidence for Neogene surface downdrop in the central Basin and Range Province: *Geological Society of America Bulletin*, v. 118, p. 475–490, doi: 10.1130/B25808.
- Horton, T.W., Sjöström, D.J., Abruzzese, M.J., Poage, M.A., Waldbauer, J.R., Hren, M., Wooden, J., and Chamberlain, C.P., 2004, Spatial and temporal variation of Cenozoic surface elevation in the Great Basin and Sierra Nevada: *American Journal of Science*, v. 304, p. 862–888, doi: 10.2475/ajs.304.10.862.
- Huber, N.K., 1981, Amount and timing of late Cenozoic uplift and tilt of the central Sierra Nevada, California—Evidence from the upper San Joaquin River basin: *U.S. Geological Survey Professional Paper 1197*, 28 p.
- Huber, N.K., 1990, The late Cenozoic evolution of the Tuolumne River, central Sierra Nevada, California: *Geological Society of America Bulletin*, v. 102, p. 102–115, doi: 10.1130/0016-7606(1990)102<0102:TLCEOT>2.3.CO;2.
- Hudson, F.S., 1955, Measurement of the deformation of the Sierra Nevada, California, since middle Eocene: *Geological Society of America Bulletin*, v. 66, p. 835–869, doi: 10.1130/0016-7606(1955)66[835:MOTDOT]2.0.CO;2.
- Hudson, F.S., 1960, Post-Pliocene uplift of the Sierra Nevada, California: *Geological Society of America Bulletin*, v. 71, p. 1547–1574, doi: 10.1130/0016-7606(1960)71[1547:PUOTSN]2.0.CO;2.
- Ingraham, N.L., and Taylor, B.E., 1991, Light stable isotope systematics of large-scale hydrologic regimes in California and Nevada: *Water Resources Research*, v. 27, p. 77–90, doi: 10.1029/90WR01708.
- Jones, C.H., Farmer, G.L., and Unruh, J.R., 2004, Tectonics of Pliocene removal of lithosphere of the Sierra Nevada, California: *Geological Society of America Bulletin*, v. 116, p. 1408–1422, doi: 10.1130/B25397.1.
- Kendall, C., and Coplen, T.B., 2001, Distribution of oxygen-18 and deuterium in river waters across the United States: *Hydrological Processes*, v. 15, p. 1363–1393, doi: 10.1002/hyp.217.
- Lindgren, W., 1911, The Tertiary gravels of the Sierra Nevada: *U.S. Geological Survey Professional Paper 73*, 226 p.
- Minnich, R.A., 2007, Climate, paleoclimate, and paleovegetation, in Barbour, M.G., Keeler-Wolf, T., and Schoenherr, A.A., eds., *Terrestrial Vegetation of California*: Berkeley, University of California Press, p. 43–70.
- Mulch, A., Graham, S.A., and Chamberlain, C.P., 2006, Hydrogen isotopes in Eocene river gravels and paleoelevation of the Sierra Nevada: *Science*, v. 313, p. 87–89, doi: 10.1126/science.1125986.
- Mulch, A., Sarna-Wojcicki, A.M., Perkins, M.E., and Chamberlain, C.P., 2008, A Miocene to Pleistocene climate and elevation record of the Sierra Nevada (California): *Proceedings of the National Academy of Sciences of the United States of America*, v. 105, p. 6819–6824, doi: 10.1073/pnas.0708811105.
- Poage, M.A., and Chamberlain, C.P., 2001, Empirical relationships between elevation and the stable isotope composition of precipitation and surface waters: Considerations for studies of paleoelevation change: *American Journal of Science*, v. 301, p. 1–15, doi: 10.2475/ajs.301.1.1.
- Poage, M.A., and Chamberlain, C.P., 2002, Stable isotopic evidence for a pre-middle Miocene rain shadow in the western Basin and Range: Implication for the paleotopography of the Sierra Nevada: *Tectonics*, v. 21, doi: 10.1029/2001TC001303.
- Roe, G.H., 2005, Orographic precipitation: *Annual Review of Earth and Planetary Sciences*, v. 33, p. 645–671, doi: 10.1146/annurev.earth.33.092203.122541.
- Roe, G.H., and Baker, M.B., 2006, Microphysical and geometrical controls on the pattern of orographic precipitation: *Journal of the Atmospheric Sciences*, v. 63, p. 861–880, doi: 10.1175/JAS3619.1.
- Rowley, D.B., Pierrehumbert, R.T., and Currie, B.S., 2001, A new approach to stable isotope-based paleoaltimetry: Implications for paleoaltimetry and paleohypsometry of the High Himalaya since the late Miocene: *Earth and Planetary Science Letters*, v. 188, p. 253–268, doi: 10.1016/S0012-821X(01)00324-7.
- Rozanski, K., Araguás-Araguás, L., and Gonfiantini, R., 1992, Relation between long-term trends of oxygen-18 isotope composition of precipitation and climate: *Science*, v. 258, p. 981–985, doi: 10.1126/science.258.5084.981.
- Scholl, M.A., Giambelluca, T.W., Gingerich, S.B., Nullet, M.A., and Loope, L.L., 2007, Cloud water in windward and leeward mountain forests: The stable isotope signature of orographic cloud water: *Water Resources Research*, v. 43, p. W12411, doi: 10.1029/2007WR006011.
- Small, E.E., and Anderson, R.S., 1995, Geomorphically driven late Cenozoic rock uplift in the Sierra Nevada, California: *Science*, v. 270, p. 277–280, doi: 10.1126/science.270.5234.277.
- Smith, R.B., 1979, The influence of mountains on the atmosphere, in Saltzman, B., ed., *Advances in Geophysics*, v. 21: New York, Academic Press, p. 87–230.
- Smith, R.B., 2003, A linear upslope-time-delay model for orographic precipitation: *Amsterdam, Journal of Hydrology*, v. 282, p. 2–9, doi: 10.1016/S0022-1694(03)00248-8.
- Smith, R.B., and Barstad, I., 2004, A linear theory of orographic precipitation: *Journal of the Atmospheric Sciences*, v. 61, p. 1377–1391, doi: 10.1175/1520-0469(2004)061<1377:ALTOOP>2.0.CO;2.
- Smith, R.B., Jiang, Q.-f., Fearon, M.G., Tabary, P., Doringier, M., Doyle, J.D., and Benoit, R., 2003, Orographic precipitation and air mass transformation: An Alpine example: *Quarterly Journal of the Royal Meteorological Society*, v. 129, p. 433–454, doi: 10.1256/qj.01.212.
- Smith, R.B., Barstad, I., and Bonneau, L., 2005, Orographic precipitation and Oregon's climate transition: *Journal of the Atmospheric Sciences*, v. 62, p. 177–191, doi: 10.1175/JAS-3376.1.
- Stock, G.M., Anderson, R.S., and Finkel, R.C., 2004, Pace of landscape evolution in the Sierra Nevada, California, revealed by cosmogenic dating of cave sediments: *Geology*, v. 32, p. 193–196, doi: 10.1130/G20197.1.

- Stock, G.M., Anderson, R.S., and Finkel, R.C., 2005, Rates of erosion and topographic evolution of the Sierra Nevada, California, inferred from cosmogenic <sup>26</sup>Al and <sup>10</sup>Be concentrations: *Earth Surface Processes and Landforms*, v. 30, p. 985–1006, doi: 10.1002/esp.1258.
- Unruh, J.R., 1991, The uplift of the Sierra Nevada and implications for late Cenozoic epeirogeny in the western Cordillera: *Geological Society of America Bulletin*, v. 103, p. 1395–1404, doi: 10.1130/0016-7606(1991)103<1395:TUOTSN>2.3.CO;2.
- Wakabayashi, J., and Sawyer, T.L., 2001, Stream incision, tectonics, uplift and evolution of topography of the Sierra Nevada, California: *The Journal of Geology*, v. 109, p. 539–562, doi: 10.1086/321962.
- Wolfe, J.A., Schorn, H.E., Forest, C.E., and Molnar, P., 1997, Paleobotanical evidence for high altitudes in Nevada during the Miocene: *Science*, v. 276, p. 1672–1675, doi: 10.1126/science.276.5319.1672.
- Wolfe, J.A., Forest, C.E., and Molnar, P., 1998, Paleobotanical evidence of Eocene and Oligocene paleoaltitudes in midlatitude western North America: *Geological Society of America Bulletin*, v. 110, p. 664–678, doi: 10.1130/0016-7606(1998)110<0664:PEOEAO>2.3.CO;2.
- Zachos, J.C., Stott, L.D., and Lohmann, K.C., 1994, Evolution of early Cenozoic marine temperatures: *Paleoceanography*, v. 9, p. 353–387, doi: 10.1029/93PA03266.
- Zachos, J.C., Pagani, M., Sloan, L., Thomas, E., and Billups, K., 2001, Trends, rhythms, and aberrations in global climate 65 Ma to Present: *Science*, v. 292, p. 686–693, doi: 10.1126/science.1059412.

MANUSCRIPT RECEIVED 8 JANUARY 2009  
REVISED MANUSCRIPT RECEIVED 20 AUGUST 2009  
MANUSCRIPT ACCEPTED 22 AUGUST 2009

Printed in the USA